Nat. Hazards Earth Syst. Sci. Discuss., https://doi.org/10.5194/nhess-2018-406
Manuscript under review for journal Nat. Hazards Earth Syst. Sci.
Discussion started: 28 January 2019

Natural Hazards and Earth System Sciences
Discussions

From examination of natural events a proposal for risk mitigation of lahars by a cellular automata methodology: a case study for Vascún valley, Ecuador

Valeria Lupiano[1,2], Francesco Chidichimo[3], Guillermo Machado[4], Paolo Catelan[3,5], Lorena Molina[4], Salvatore Straface[3], Gino M. Crisci[1], Salvatore Di Gregorio[6,7]

[1]Department of Biology, Ecology, Earth Sciences, University of Calabria, Arcavacata, 87036 Rende, Italy
[2]Consiglio Nazionale delle Ricerche, CNR-IRPI, Via Cavour 6, 87030 Rende, CS, Italy
[3]Department of Environmental and Chemical Engineering, University of Calabria, Arcavacata, 87036 Rende, Italy
[4]Faculty of Engineering, National University of Chimborazo, Riobamba, Ecuador
[5]CEAA - Centro de Energías Alternativas y Ambiente,Escuela Superior Politécnica del Chimborazo, Riobamba, Ecuador
[6]Department of Mathematics and Computer Science, University of Calabria, Arcavacata, 87036 Rende, Italy
[7]ISAC - CNR, Lamezia Terme, Zona Industriale 88046 Lamezia Terme, CZ, Italy

Correspondence to: Francesco Chidichimo (francesco.chidichimo@unical.it)

Abstract. Lahars are erosive floods, mixtures of water and pyroclastic deposits, they look the biggest environmental disaster as number of fatalities in the volcanic areas. Security measures have been recently adopted in the threatened territories, by constructing retaining dams and embankments in key positions. Such solutions could involve a strong environmental impact for the works and the continuous accumulation of volcanic deposits, such that equilibrium conditions could lack far, triggering more disastrous events. An improved version of the Cellular Automaton model LLUNPIY for lahars simulations is presented. The growing frequency of lahars, maybe for the climatic change, in the Vascún Valley of Tungurahua Volcano, Ecuador has recently produced smaller and less dangerous events, sometimes favoured by the collapse of temporary ponds, generated by small landslides. An investigation is here performed in order to reproduce such situations in controlled way by the use of LLUNPIY simulations. Using precise field data, points are individuated where dams by backfills, easy to collapse, can produce momentary ponds; LLUNPIY simulations permit to project triggering of small lahars by minor rainfall events or to project in the case of larger rainfalls the anticipation of lahar detachment, avoiding simultaneous and dangerous confluence with other lahars.

1 Introduction

Lahars are one of the most devastating phenomena as amount of fatalities in volcanic areas. They are flows, other than common stream flow, and consist of pyroclastic deposits mixed to water. Their physical properties (density, viscosity, consistency) are very similar to wet concrete not yet hardening (Vallance, 2000). This fluid, under steep slopes conditions, is capable of reaching speeds up to100 km/h and distances up to 300 Km, it becomes solid when water is gradually released in flat areas, (Manville et al., 2013).

Lahars may be of primary type (or syneruptive) if directly related to volcanic eruptions, usually when glacier and/or snow are melt by pyroclastic or lava flows, lahars develop from mixing pyroclastic matter with water as the tremendous 1985 Colombian event of Nevado del Ruiz (Pierson et al., 1990); another case could occur when a large quantity of water is available by the breakout of a natural lake because of eruption (Manville, 2010).

Secondary lahars are produced when a largest water quantity is available directly by extreme meteorological events or indirectly by the overflow of superficial water bodies. Pyroclastic matter of previous eruptive activity is mobilized, e.g., the pyroclastic flows of Mt. Pinatubo, 1991 Philippines (Rodolfo et al., 1996).

Soil erosion with water incorporation along streams increases the volume of both primary and secondary lahars.

Two main triggering mechanisms are possible:

a) process of mobilization related to pyroclastic sediments sometimes mixed with some exotic material (tephra): if superficial water amount overcomes a threshold, related to features of pyroclastic stratum and soil slope, then the percolation can cause a detachment in the unconsolidated stratum;

b) process of erosion, depending mainly on the redistribution of volcanic sediment along the slopes (Leavesley et al., 1989; MAJOR et al., 2000): in fact unconsolidated tephra in surface is swept away by flows, mixing with water and gradually enlarging their volume because of contribution of both sediments and waters (Barclay et al., 2007).

Different approaches were considered in literature for modelling lahars: empirical models (e.g. Schilling, 1998; Muñoz-Salinas et al., 2009) were developed, accounting mainly for some phenomenological macro-observables, simplified hydrological and rheological models that reduce the lahar behavior to a Newtonian-like behavior (e.g. O'brien, 1993; Costa, 1997), numerical methods approximating PDE (e.g. Pitman et al., 2003); Cellular Automata (CA) alternative methodology for lahar modelling will be exhibited later.

In many issues of various disciplinary backgrounds, but regarding complex systems, research was able of progress thanks to computer simulations, permitting to develop multidisciplinary and transdisciplinary approaches, linked in part to the emergence of alternative computing paradigms, such as CA (Toffoli, 1984, Chopard, 1998, Iovine et al., 2007).

CA themselves are a complex dynamic system that is “merged” in a discretized space/time. Space is regularly tessellated in cells; an identical input/output computing device (a Finite-State Machine, FSM, called also finite-state automa) is assigned to each cell; the output corresponds to the state of the cell, the input is given by the states of the cells of the “neighborhood”, that is specified by a pattern, that is constant in space and time. Complex dynamic systems, whose evolution depends exclusively on local interactions of their elementary components, may be usually well modelled by CA, that share the same feature of localism or acentrism (Chopard, 1998).

CA applications may be extended to more complex systems, if the primitive definitions are expanded in order to capture a broader phenomenology: Multicomponent (more known as Macroscopic) Cellular Automata (MCA) account for phenomena, whose dynamics involves more interacting processes, often of different nature, furthermore in particular conditions the prerequisite of localism for a process may be weakened. This implies that the transition function has to be divided in parts, the “elementary processes”, that are computed sequentially, each one involves the updating of the MCA states; furthermore

the not local processes are introduced in MCA as "external influences", they account for kinds of input from the "external world", sometime of probabilistic type, e.g. raining, distribution of pyroclastic bombs during an eruption. A MCA step occurs when all the elementary processes and the functions related to "external influences" (Di Gregorio and Serra, 1999) are executed.

A complex phenomenology can imply that the state has to account for very different features of the space physically corresponding to the cell; this involves that the state is defined by substates (e.g., the temperature, depth of pyroclastic stratum). The introduction of the substates involves an important advantage when surface phenomena are considered: features related to the third dimension may be expressed in terms of substates, it permits to develop two dimensions models, operating three-dimensionally in fact (Avolio et al., 2012).

Simulations of flow-like landslides were performed by several versions of the MCA model SCIDDICA since 1987 for both subaerial and subaqueous debris/granular/mud flows (e.g., Barca et al., 1987; Avolio et al. 2008; Mazzanti et al., 2010; Avolio et al. 2013; Lupiano et al., 2014; Lupiano et al., 2015a; Lupiano et al., 2015b; Lupiano et al., 2015c; Lupiano et al., 2017). Simulations of primary and secondary lahars were performed by the MCA model LLUNPIY (Machado et al., 2014; Machado et al., 2015a; Machado et al., 2015b; Chidichimo et al., 2016).

LLUNPIY, SCIDDICA-SS3 and SCIDDICA-SS2 are our top models for simulating flow-like landslides and lahars, they permit to simulate the erosion process unlike other models, that were used in lahar simulation: LAHARZ (e.g., Schilling, 1998; Muñoz-Salinas et al., 2009), TITAN2D (e.g., Sheridan, 2005; Williams, 2008; Córdoba et al., 2014).

Reliable simulation tools are very important in order to organize security measures and test them in different conditions by computers, even if such instruments have to be used with extreme caution, because the complex problem of lahar hazard must be studied from an interdisciplinary way (Lane et al., 2003; Leung et al., 2003), safety measures can increase the disaster risk in several conditions.

Beside tools of early warning, which could work only partially, beside temporary or definitive land evacuation which could involve a strong social impact and economic destitution, security measures have been adopted in volcanic territory, by constructing retaining dams, embankments, walls, dykes, levees, reservoirs in key positions for containing and deviating possible lahars (Scott, 1989; Verstappen, 1992; Aguilera, 2003; Künzler et al., 2012; Carey et al., 2012). This solution could involve a strong environmental impact both for the works and the continuous accumulation of volcanic deposits, such that equilibrium conditions could lack far, triggering more disastrous events (Janda et al., 1981, 1996; Scott, 1989; Procter et al., 2010).

The growing frequency of lahars in the area of Vascún Valley of Tungurahua Volcano, Ecuador, maybe for the climatic change, has recently produced smaller (shorter accumulation periods) and therefore less dangerous events (Mothes and Vallance, 2015). Moreover, small landslides, forming natural dams with temporary ponds, could easily trigger lahars by collapsing because of rainfalls; it sometime happens, e.g. the IGEPN (Instituto Geofísico Escuela Politecnica Nacional, Quito, Ecuador) reported such a case of August, 23 2008 (2008a; 2008b).

The use of simulation tools (from the cellular automata model LLUNPIY) needs detailed field data: DTM, depth of erodible pyroclastic stratum. It implies accurate geological investigations, including subsoil tomographies; permitting to individuate points, where dams by backfills, easy to collapse, can produce momentary ponds, whose breakdown can trigger a lahar (Machado, 2015c; Chidichimo et al., 2016).

For such points, minor rainfall events can produce small lahars, major events will anticipate the lahar detachment, avoiding simultaneous confluence with other lahars. The control of the discharge channels could permit in various situations many combinations for a controlled triggering of lahars, in order to mitigate the lahar risk.

The next chapter is devoted to the geological description of the Vascún Valley, the third chapter introduces LLUNPIY, the MCA model for simulating primary and secondary lahars, together with its validation in simulating some significant lahars of Vascún Valley. In the fourth chapter, the building of dams, easy to collapse, with discharge channel is considered, then favorable locations of dams are hypothesized for a controlled triggering of lahars, of which effects are simulated for possible events; at the end, conclusions and comments.

2 Geological setting of Vascún valley

Tungurahua is one of the most active and dangerous volcanoes in the Ecuadorian Andes (Cordillera Oriental) on the inside of the Sangay National Park; its summit, 5023 m.a.s.l., is positioned at longitude 78° 27’ W, latitude 01° 28’ S. It a stratovolcano, whose evolution involved the succession of three major volcanic edifices (Tungurahua I, Tungurahua II, Tungurahua III) since the mid-Pleistocene over a basement of metamorphic rocks. Historical eruptions have all originated from the summit crater. The main events of eruptive activity occurred between: 1640–1641, 1773–1777, 1886–1888, 1916–1918 and from 1999 until the present (Hall et al., 1999; Ramón, 2009; Biggs et al., 2010). The average of eruptions in the last two thousand years is once per century according to the detailed studies of Le Pennec et al. (2008). They have been accompanied by strong explosions and sometimes by pyroclastic flows and lava flows that reached populated areas at the volcano's base. The formation of rain-induced lahar is also a cause of danger. Approximately 32,000 live within the higher risk areas, mainly in rural villages and in the touristic (thermal springs) town of Baños de Agua Santa (Mothes et al., 2015). Baños de Agua Santa (1800 m.a.s.l.) is only 8 Km as the crow flies away from the summit; 30 Km to NW, 30 km to SW and 140 km to N are the distances respectively from the towns of Ambato, Riobamba, and from the capital Quito.

Nat. Hazards Earth Syst. Sci. Discuss., https://doi.org/10.5194/nhess-2018-406
Manuscript under review for journal Nat. Hazards Earth Syst. Sci.
Discussion started: 28 January 2019

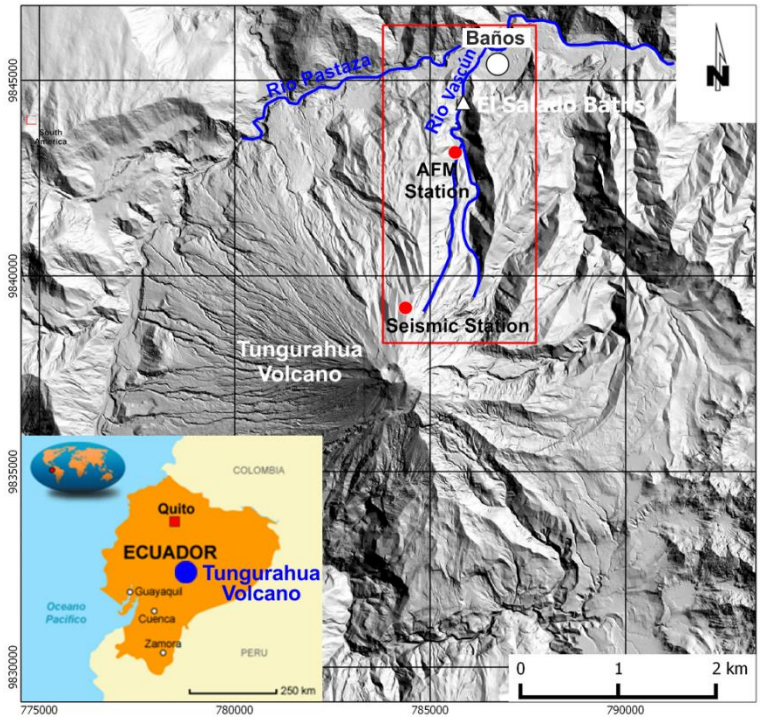

Figure 1: Tungurahua Volcano. The Vascún Valley is inside the red box.

The small glacier of Tungurahua volcano is reduced both for the global warming phenomenon and for the intensification of the volcanic activity after the 1999, therefore the today snow cover is completely negligible for generating primary lahars, consequently triggering of lahars with significant frequency and magnitude, is subordinated both to the intensity and duration of the rainfalls and the available quantity of fresh material along the slopes and within the principal canyons (Quebradas of the Rio Vascún, Juive Grade-La Pampa Valley, Achupashal Quebrada) and in a minor from other factors. Almost all the lahars are confined to the canyons and converge into Pastaza River (Mothes and Vallance, 2015).

In fact, eruptive activity of Tungurahua volcano, during last years, has generated greater availability of pyroclastic debris that is periodically remobilized from atmospheric phenomena, often not particularly violent but prolonged for several days. Between 2000 and 2011, around 900 events rain-induced lahars were triggered (Mothes and Vallance, 2015).

Generally, lahars magnitude is small and, consequently, causes limited damage. IGEPN, and its Acoustic-Flow-Monitor (AFM) station, which monitors passing of secondary lahars, detects most of lahars, while many others are traced by the Observatory of the Volcano Tungurahua (OVT), which is situated 13 km to the north-northwest of the crater, also with the observation contribution of local volunteers (vigias).

2.1 The 2008 secondary lahars of Vascún Valley

Rio Vascún, the most important river in the area, gave its name to the Valley on the NE flank of Tungurahua Volcano, it flows into the Rio Pastaza (Fig.1). The valley slopes exceed 35°-40°in the first steepest 3 km, while range from 20° to 6° in

Nat. Hazards Earth Syst. Sci. Discuss., https://doi.org/10.5194/nhess-2018-406
Manuscript under review for journal Nat. Hazards Earth Syst. Sci.
Discussion started: 28 January 2019

the last less steeply 2-3 Km. Furthermore, the path of Rio Vascún is extremely sinuous in the upper 1-2 km of terraces, the river is there characterized by a succession of tight 90° bends.

The Vascún Valley is highly susceptible to lahar flows that threaten the nearby populated areas which were inundated several times in the past years: the town of Baños, that extend in part of the depositional area, was affected several times, the thermal structure "El Salado", that is located along the river banks, had been repeatedly damaged by passage of lahars (Fig. 2),

On August 13 2008 at an elevation of about 2200 m a.s.l., a small landslide produced a natural dam along Rio Vascún. The dam originated a pond with a length of 100 m, a depth of 3 m and a width of 20 m. After heavy rains on August 22, the dam collapsed and generated a lahar. The flow velocity was estimated in 15 m/s with a flow rate of 1120 m^3/s and an average height of 4 m (IGEPN, 2008a and 2008b), this flow rate is ten times greater than that recorded in 2005 event (IGEPN, 2005, Williams et al., 2008). The lahar reached in 5 minutes El Salado and devastated the pools of the thermal spa, afterwards destroyed further downstream some houses of Las Ilusiones (a village of Baños district).

Figure 2: a) Google Earth view of Tungurahua Volcano with indication of main localities of the study area; b) lahar at thermal structure of "El Salado".

Nat. Hazards Earth Syst. Sci. Discuss., https://doi.org/10.5194/nhess-2018-406
Manuscript under review for journal Nat. Hazards Earth Syst. Sci.
Discussion started: 28 January 2019

3 LLUNPIY model for lahar simulation

LLUNPIY (Lahar modelling by Local rules based on an UNderlying PIck of Yoked processes, "llunp'iy" means flood in the Quechua language) is a model for simulating secondary and primary lahars according to MCA methodology applied to complex system, whose evolution may be mainly specified in terms of local interaction. MCA features of SCIDDICA-SS3 (Avolio et al., 2013) and SCIDDICA-SS2 (Avolio et al., 2008; Lupiano et al., 2016; Lupiano et al., 2017) are inherited by LLUNPIY; LLUNPIY for secondary lahars is extensively defined in Machado et al. (2015b), here are reported only the features of the model, that were applied in the study cases (reduced version LLUNPIY/3r from SCIDDICA-SS2), where the initial phase is abrupt, it is given by the temporary pond collapse without water percolation and detachment subsequent to water inclusion, furthermore in the simulation of real and hypothesized events, all the lahars end into the Rio Pastaza, so the last phase of lahar deposition is omitted. LLUNPIY modelling of water percolation and water extrusion with pyroclastic debris deposition can be found also in Machado (2015c).

3.1 Introduction to the LLUNPIY/3r version

The following quintuple defines the two-dimensions (with hexagonal cells) MCA model LLUNPIY/3r

$$<T, P, N, Q, \sigma>$$

where:

- $T = \{(x, y) \mid x, y \in \mathbb{N}, 0 \leq x \leq l_x, 0 \leq y \leq l_y\}$ is the set of hexagonal cells, that tessellated the territory, where the phenomenon evolves; the cells are individuated by the points with integer co-ordinates (Fig.3, left) of their centers; $\mathbb{N}$ is the set of the natural numbers.
- P is the set of the both empirical and physical global parameters, they are related to the global common features of the phenomenon (Table 1);
- $N = <(1,-1), (0,-1) (-1,0), (-1,1), (0,1), (1,0), (0,0)>$ the neighborhood index, identifies the geometrical pattern of cells (Fig.3, right), which influence the state change of the "central" cell; index 0 is assigned to the central cell and indexes 1,..,6 are assigned to the six adjacent cells; $\#N=7$.
- Q is the finite set of states of the finite states machine (or automaton), incorporated in the cell; it is specified in terms of substates as their Cartesian product (Table 2).
- $\sigma : Q^{\#N} \rightarrow Q$ is the deterministic transition function for each cell in T, the following "elementary" processes compose σ, they account for the overall dynamics of the phenomenon:
    - τ_{mob}, effects of mobilization
    - τ_{lo}, lahar outflows
    - τ_{te}, effect of turbulence
    - τ_{fc}, composition of flows

Nat. Hazards Earth Syst. Sci. Discuss., https://doi.org/10.5194/nhess-2018-406
Manuscript under review for journal Nat. Hazards Earth Syst. Sci.
Discussion started: 28 January 2019

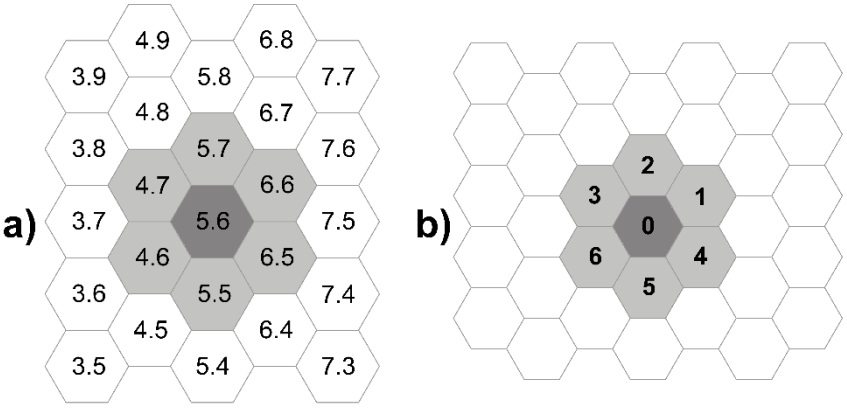

Figure 3: a) The neighborhood of cell (5,6); b) neighborhood indexes.

3.2 The elementary processes of LLUNPIY/3r

We give in the following an outline of the of the transition function, by the elementary processes, each one updating the sub-states, in order to capture the mechanisms; the complete execution of the function "external influence" and all the elementary processes complete a step of the MCA. Neighborhood index between square brackets, following substate specification, indicates the corresponding cell of the neighborhood. ΔQ_S indicates variation of the sub-state Q_S. Q'_S indicates the new value of the substate Q_S.

Pyroclastic cover mobilization

Soil features together with the quantity of water content determine a value p_{tm} of mobilization threshold to be compared with the kinetic head Q_{KH} of lahar debris inside the cell, when $Q_{KH} > p_{tm}$, then the pyroclastic cover is eroded, the lahar thickness augments and altitude diminishes according to the following formula

$$-\Delta Q_D = \Delta Q_{TH} = -\Delta Q_A = (Q_{KH} - p_{tm}) \cdot p_{pe}\,, \tag{1}$$

There is correspondingly a dissipation of energy with a decrease of kinetic head according to the following formula:

$$-\Delta Q_{KH} = (Q_{KH} - p_{tm}) \cdot p_{de}\,, \tag{2}$$

Effect of turbulence

A loss of kinetic head occurs by turbulence at each LLUNPIY step according to the following equation:

$$-\Delta Q_{KH} = p_{dt} Q_{KH} \tag{3}$$

Lahar outflows

$f[i], 1 \le i \le 6$, specify the outflows from the central cell toward the adjacent cell, $f[0]$ is the part remaining in the central cell. They are computed is in two steps: application of the Algorithm of the Minimization of Differences, AMD (Avolio *et*

Nat. Hazards Earth Syst. Sci. Discuss., https://doi.org/10.5194/nhess-2018-406
Manuscript under review for journal Nat. Hazards Earth Syst. Sci.
Discussion started: 28 January 2019

Natural Hazards and Earth System Sciences
Discussions

al., 2012; Di Gregorio and Serra, 1999) to the "heights" in the neighborhood of the central cell and calculation of the shift of the outflows (Avolio *et al.*, 2013).

AMD application computes the outflows, that minimize the "height" differences in the neighborhood (equation 7). An alteration of height values is introduced in the central cell for taking into account the outflow run-up; furthermore the viscosity is modelled by an adherence "adh" term, the lahar quantity, that cannot leave the central cell. It varies between the two extreme values $adh1$ and $adh2$, which depend on the composition of the pyroclastic debris at the maximum and minimum water content (Machado, 2015c).

$$h[0] = Q_A[0] + Q_{KH}[0] + adh\,, \tag{4}$$

$$h[i] = Q_A[i] + Q_{TH}[i], (1 \le i \le 6)\,, \tag{5}$$

$$q = Q_{TH}[0] - adh = \sum_{0 \le i \le 6} f[i] \tag{6}$$

$$\sum_{\{(i,j)/0 \le i < j \le 6\}} (|(h[i] + f[i]) - (h[j] + f[j])|) \tag{7}$$

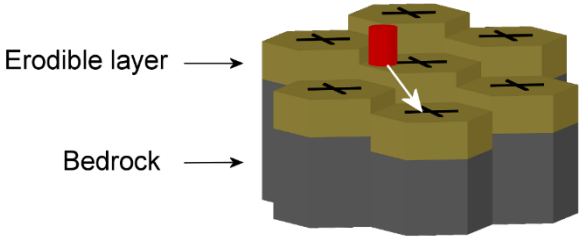

Figure 4: Outflow direction from central cell to the center of an adjacent cell in 3-dimensions.

Each moving quantity (outflow) may be considered as a "cylinder", that initially is entirely inside the cell, having a center of mass with co-ordinates of $Q_X[0]$and $Q_Y[0]$ and with the maximum possible radius.

The shift "$sh[i]$" of $f[i]$ is calculated according to the following formulae, where the movement of the mass center is specified as the mass movement on a constant slope with a constant coefficient of friction p_{cf}, the movement of $f[i]$ is directed towards the center of cell i, considering the slope angle $\theta[i]$ (Fig.4).

$$sh[i] = v \cdot p_t + g(sin\theta[i] - p_{cf} cos\theta[i])\, p_t^2/2\,,\ (1 \le i \le 6)\,, \tag{8}$$

with "g" the acceleration of gravity, "v" the initial velocity:

$$v = \sqrt{(2g \cdot Q_{KH}[0])} \tag{9}$$

There are three possible outcomes: if the shifted cylinder is completely inside (outside) the central cell, there is only an internal (external) outflow, otherwise two cylinders form with mass center corresponding to the mass center of the internal outflow and of the external outflow. The new position of external and internal outflow accounts also for the variation of kinetic head.

Nat. Hazards Earth Syst. Sci. Discuss., https://doi.org/10.5194/nhess-2018-406
Manuscript under review for journal Nat. Hazards Earth Syst. Sci.
Discussion started: 28 January 2019

Natural Hazards and Earth System Sciences Discussions

Flows Composition

Execution of the elementary process "lahar outflows" involves an updating of substates Q_{LT}, Q_{KH}, Q_X, Q_Y by the elementary process "Flows Composition". It accounts for the loss of matter (Q_{LT}) and corresponding variation of Q_{KH}, Q_X, $Q_Y$that is determined by the external outflows, while internal outflows don't effect a loss of matter, just a shift, that determine still variations of the other previously quoted substates; inflows are determined by possible outflows of the neighbor cells towards the central cell (Machado et al., 2015).

3.3 Simulations of 2008 lahars of Vascún valley

We selected the 2005 and 2008 lahars of Vascún Valley for LLUNPIY simulations, because available (although incomplete) data of the flood phase (Machado et al., 2015b) would allow reliable simulations. Data of different sources were carefully compared and analyzed (Williams et al., 2008; IGEPN, 2008) in order to reconstruct as accurately as possible the two events (Machado et al., 2014a and 2014b).

The same set of LLUNPIY parameters was used in the two cases except for the parameter of progressive erosion (*ppe*) because of different percentages of water in the soil. The 2005 event was triggered in a higher zone of Rio Vascún, when the water concentration in the soil by rainfall reached critical values in areas, where a slope threshold was exceeded. The 2008 event was dissimilar, because the breaking of a temporary pond released suddenly a larger water quantity (in comparison with 2005 case) with strong turbulence, whose effects correspond to a higher value of the parameter of progressive erosion (Machado et al., 2015b).

Here, we report extensively the results of simulations of 2008 event of the Vascún Valley in Machado et al. (2015b), because the causes of this event are given by a breaking of a temporary pond, that is the same phenomenology, whose development, we want to forecast. The reliability of results of the simulation in comparison with the real event permitted us to confide in the goodness of the method, the new simulations were performed with the same data precision and the same values of parameters.

2008 pre-event morphological data are founded on a DEM, 5 m cell size, furthermore a constant depth of 5 m was presumed for pyroclastic stratum, because of lack of detailed surveys. So approximations, that affect simulations, are introduced. Such approximations can be reduced by an opportune survey of field data, e.g. by soil tomographies.

The simulation of the 2008 lahar is shown in Fig. 5: the flow speed arrived up to 20 m/s in many areas of the valley, about 970000 m^3 is the quantity of eroded material. The maximum height obtained in the simulated flow (Fig. 6a) is 22 m and has been reached in some sectors where the valley is particularly narrow, while the estimated average value by IGPEN (2008a and 2008b) is 4 m.

Table 3 compares some data of simulation by LLUNPY with corresponding field data of IGEPN (2008). It is possible to note that the data deriving from the simulations are not many different from the known measured ones. The flow velocity of 15

Nat. Hazards Earth Syst. Sci. Discuss., https://doi.org/10.5194/nhess-2018-406
Manuscript under review for journal Nat. Hazards Earth Syst. Sci.
Discussion started: 28 January 2019

m/s represents an estimated value, not measured. These results demonstrate that LLUNPIY is a reliable model, if we take into account that simulation are based on incomplete, sometime very approximate data concerning the pre-event and post-event, furthermore the inevitable errors in records related to this event have to be considered. Therefore an extension of LLUNPIY/3r is promising in order to introduce secondary phenomenological features to be tested. Simulations reproduce satisfactorily the overall dynamics of the events; there is a good matching between real and simulated lahar path, velocity and height of detrital flow; note that different approaches obtain always excellent results about the path because the lahar is canalized by steep faces.

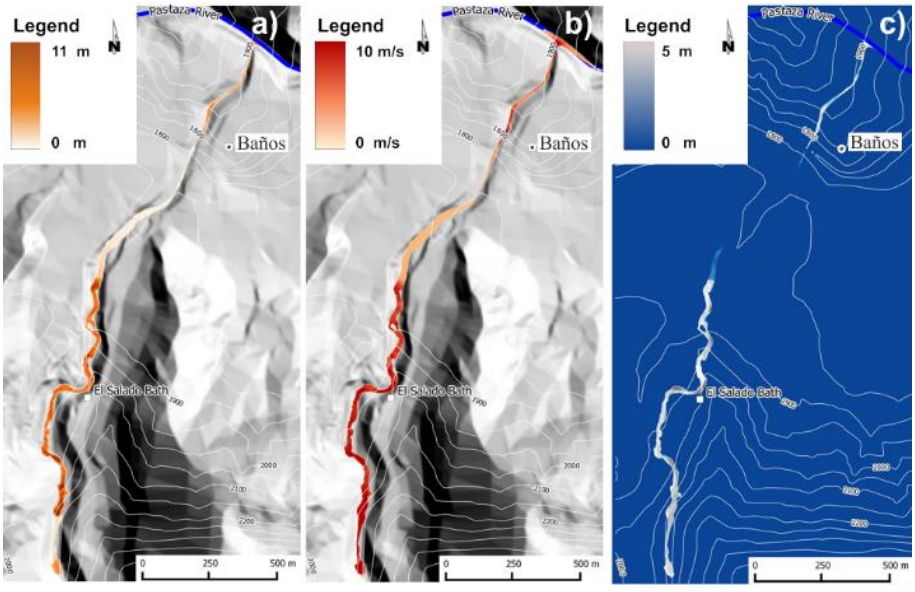

Figure 5: 2008 simulated event. a) Maximum thickness, b) Maximum velocity, and c) erosion depth.

4 Lahar triggering and effects

4.1 Building rudimental dams easy to collapse

Momentary ponds form along watercourses in volcanic areas, when landslides of volcanic deposits, which are originated by pyroclastic flows and lahars, act as a dam by obstructing the stream bed. The most frequent cause of a breakout of such natural ponds is the overflow of water across the newly formed dam during violent rainfalls and subsequent erosion and rapid cutting down into the loose rock debris. The classification of the "Glossary of Meteorology" of the American Meteorological Society for rainfall intensity (Glickman, 2000) is here adopted according to the rate of precipitation R_p: measured in mm h^{-1}:

Light rain: $R_p < 2.5$ mm h^{-1};

Moderate rain: 2.5 mm $h^{-1} \leq R_p < 10$ mm h^{-1};

Heavy rain: 10 mm $h^{-1} \leq R_p \leq 50$ mm h^{-1};

Violent rain: $R_p > 50$ mm h^{-1}.

Dam collapse occurs when instability conditions arise in the downstream slope. By eroding the obstruction and flowing downstream along the river bed, the initial surge of water will incorporate a dangerous volume of sediments. This can easily produce lahars with possible devastating effects for settlements in their path (Leung et al., 2003).

Temporary dams with a similar (but controlled) behavior can be designed and built at low cost by local backfills in order to allow the outflow of streams produced by regular rainfall events. This result is achieved by properly dimensioning the embankment according to a stability analysis. The latter is made by comparing the forces tending to cause movement of the mass of pyroclastic material (force of water) with those tending to resist the movement (soil strength) (Lambe and Whitman, 1979). The aforementioned approach is traditionally adopted to prevent dams failure, but it will be used, in this case, to ensure their collapse at a fixed water level.

The Finite Element Method (FEM) was applied to perform the downstream slope stability analysis. The shear strength reduction (SSR) approach, which is one of the most popular techniques to perform FEM slope analysis, was adopted (Griffits et al., 1999). The SSR is simple in concept: it systematically reduces the shear strength envelope of material by a factor of safety (FS), and computes FEM models of the slope until deformations are unacceptably large or solutions do not converge. In classical soil mechanics, the factor of safety is the ratio of the shear strength at the plane of potential failure τ_f and the shear stress acting in the same plane τ, namely:

$$FS = \tau_f / \tau \tag{10}$$

For the Mohr–Coulomb criterion, the previous equation reads:

$$FS = (c + (s_n - u) \cdot tan\phi)/\tau \,, \tag{11}$$

where c is the cohesion and ϕ is the friction angle of the material, s_n denotes the total normal stress and u the pore pressure. For the Mohr–Coulomb model, a "reduced" set of material parameters c^* and ϕ^* is computed:

$$c^* = c/FS_n \,, \tag{12}$$

$$tan\phi^* = tan\phi/FS_n \tag{13}$$

The problem is then solved using this set of reduced material parameters while keeping all other parameters unchanged. If convergence is obtained, the FS_n value is increased and the problem is solved again. The lowest FS_n producing non-convergence is reported as the "factor of safety" of the problem. If the resulting FS is greater than one, for a given water level stressing the upstream slope of the dam, the structure is stable. If the iterative procedure gives back a unitary FS value, the limit equilibrium conditions have been reached. This means that the coupling of both the dam geometrical configuration and the water level situation are going to produce the collapse of the structure. This last condition is the one that must be reached for the study purposes. The pore pressure distribution inside the dam body is a fundamental input for the strength

reduction analysis. Such distribution is obtained as a function of the hydraulic head stressing the upstream slope of the embankment. The filtration process, implemented in the finite element model, is based on the solution of the Laplace equation (Molinari et al., 2014; Chidichimo et al., 2015; Chidichimo et al., 2018):

$$\nabla^2 h = 0\,, \tag{14}$$

where $h(x, y)$ represents the hydraulic head distribution within the dam body which is a function of the hydraulic conductivity of the dam material. Such dependence is defined by Darcy's law:

$$q = -K\nabla h = -K\,\frac{d}{dl}\left(\frac{u}{\rho g} + z\right), \tag{15}$$

where q is Darcy's velocity, K is the hydraulic conductivity, ρ is the water density, u is the pore pressure and z is the elevation above sea level. Several simulations were performed taking the parameters for the numerical model from the literature. Studies performed on the geotechnical properties of the volcanoclastic formation that is found in the Andes of Ecuador and Colombia, known as Cangahua, reported that the dry unit weight of the material was found to range around 14 kN m^{-3} (Bommer et al., 2002). The strength parameters of volcanic sediments produced by recent eruptions were investigated by Orense et al., (2006), who found a value for the friction angle (ϕ) of these materials of about 40°, while the cohesion (c) is close to zero. The hydraulic conductivity (K) of pyroclastic beds was discovered to range between 10^{-4}-10^{-5} m s^{-1} (Burgisser, 2012). A middle range value was adopted to implement the numerical models. The relatively high permeability of the pyroclastic material ensures the water outflow during the regular rainfall regimen. In case of extreme rainfall events (violent rains, typhoons, etc.), the volcanic material is no longer able to drain the water inflow producing the water level raising which will undermine the structure stability. The dams were thought to reach a height of 3 m and to hold out up to a maximum water level of 2.6 m. Assuming the aforementioned features, the first step started from the design of a stable dam configuration (Fig. 6a). This outcome was obtained trying different dimensioning solutions in order to avoid the early collapse of the structure due, for example, to its own weight. Figure 6b shows the water velocity field in the dam cross section, while Fig. 6c shows the failure surface in the downstream slope which is generated by a factor of safety of 1.28.

Nat. Hazards Earth Syst. Sci. Discuss., https://doi.org/10.5194/nhess-2018-406
Manuscript under review for journal Nat. Hazards Earth Syst. Sci.
Discussion started: 28 January 2019

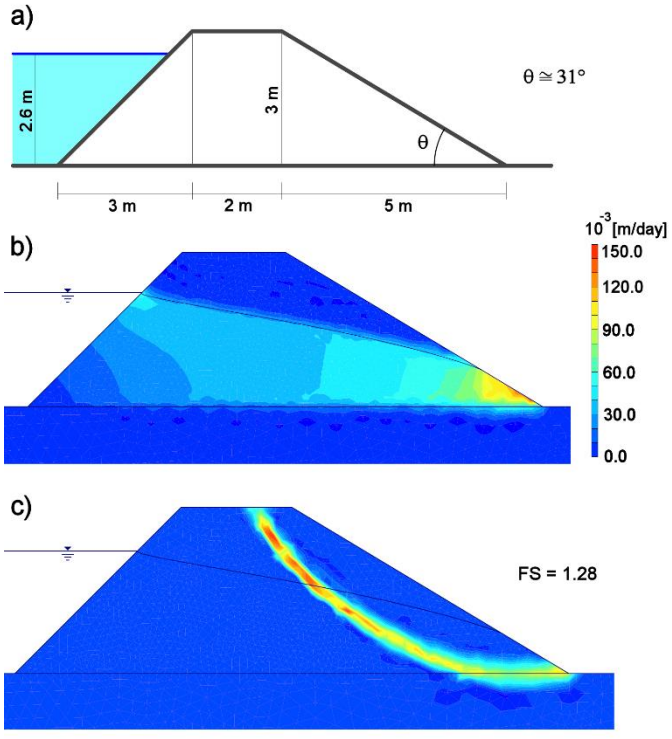

Figure 6: - a) cross sectional sketch of a stable dam with the main elements dimension; b) water velocity field moving in the dam body and associated phreatic surface; c) failure surface generated by a factor of safety of 1.28.

Once a stable dam was obtained for the chosen working conditions, the second step was to repeat the strength reduction analysis several times by slowly increasing the inclination of the downstream slope until a unitary *FS* was reached. The inclination was increased using the corner between the downstream slope and the dam crest as a pivot point. This resulted in a gradual increase of the θ angle and a consequent reduction of the dam base. Figure 7 shows the analysis final result with the sizing specifications for an easy to collapse dam built in volcanoclastic material. To ensure a greater control over the natural dam collapse timing, a discharge channel can be arranged at the dam base. The degree of openness of this channel can be adjusted according to the flow rates values observed during the extreme rainfall events recorded over time in the area, in order to delay the achievement of the triggering hydraulic head. This ploy may be necessary to avoid the undesired simultaneous collapse of different dams; hazard could increase when different lahars are triggered at short time intervals and reach the confluence points almost at the same time.

Nat. Hazards Earth Syst. Sci. Discuss., https://doi.org/10.5194/nhess-2018-406
Manuscript under review for journal Nat. Hazards Earth Syst. Sci.
Discussion started: 28 January 2019

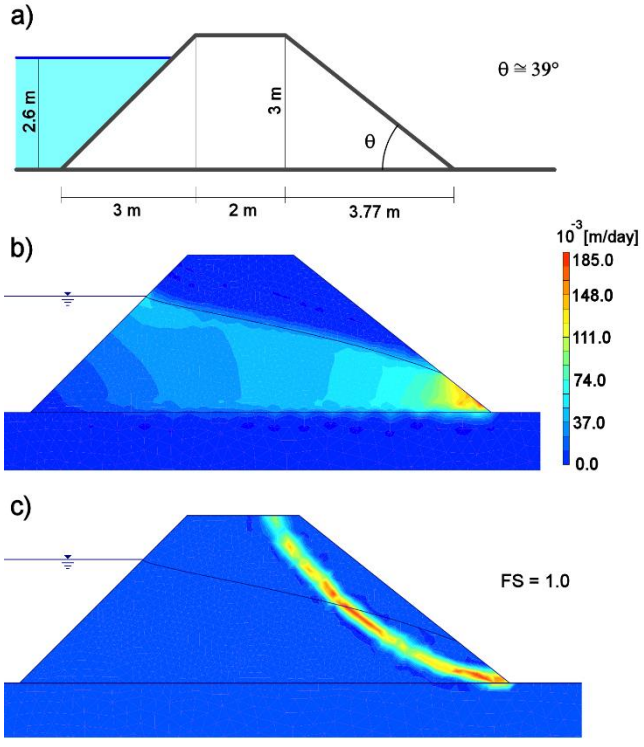

Figure 7: a) cross sectional sketch of an instable dam with the main elements dimension; b) water velocity field moving in the dam body and associated phreatic surface; c) failure surface generated by a unitary factor of safety.

4.2 Preliminary hypotheses and results of simulations

LLUNPIY was validated for secondary lahars by simulating two events of February 12, 2005 and August 22, 2008 in the Vascún Valley of Tungurahua Volcano in Ecuador (Machado et al., 2014; Machado et al., 2015b). In particular, the 2008 event is very important in order to confirm the value of the model parameters, tuned in the simulation even where the cause of the lahar was the breakdown of a temporary pond, generated by a small landslide. Those successful simulations permitted to be confident in the scenarios which could be realized by new simulations. Of course, a very accurate updating of geological data (DEM or DTM, detrital cover depth, etc.) and sufficient soil tomographies are necessary for applications in order to mitigate the lahar risk.

An initial study was performed about the potentiality of applying security measures in the Vascún Valley by triggering lahars of planned size (the lahar level is here considered as the relevant datum) through the controlled collapse of rudimentary ponds.

A preliminary analysis of the principal canyons of the Vascún Valley was performed in order to individuate favorable points for positioning embankments as dams; three points were chosen for building temporary dams: one located into Rio Vascún (1 in Fig. 8, Fig. 9, Fig.10), the second one located in a stream, tributary from the right (2 in Fig. 8, Fig. 9, Fig. 10), the third one located in a stream, tributary from the left (3 in Fig. 8, Fig. 9, Fig. 10). Rio Vascún in turn is tributary of much broader

Nat. Hazards Earth Syst. Sci. Discuss., https://doi.org/10.5194/nhess-2018-406
Manuscript under review for journal Nat. Hazards Earth Syst. Sci.
Discussion started: 28 January 2019

Natural Hazards and Earth System Sciences
Discussions

Pastaza River, where lahars of Vascún Valley disperse. Simulations concern the lahars generated in the points 1, 2 and 3 (Fig. 8, Fig. 9, Fig. 10), in short, lahar 1, 2 and 3. The same initial volume of 2008 event was selected for all the simulations except the last one. Three initial points permit to analyze an almost exhaustive set of possible conditions; we performed a sequence of simulations by LLUNPIY, of course, with the same parameters values of the successful simulation of 2008 August 29 event. We present here some selected simulations, which look interesting for many considerations, which may be deduced by their analysis.

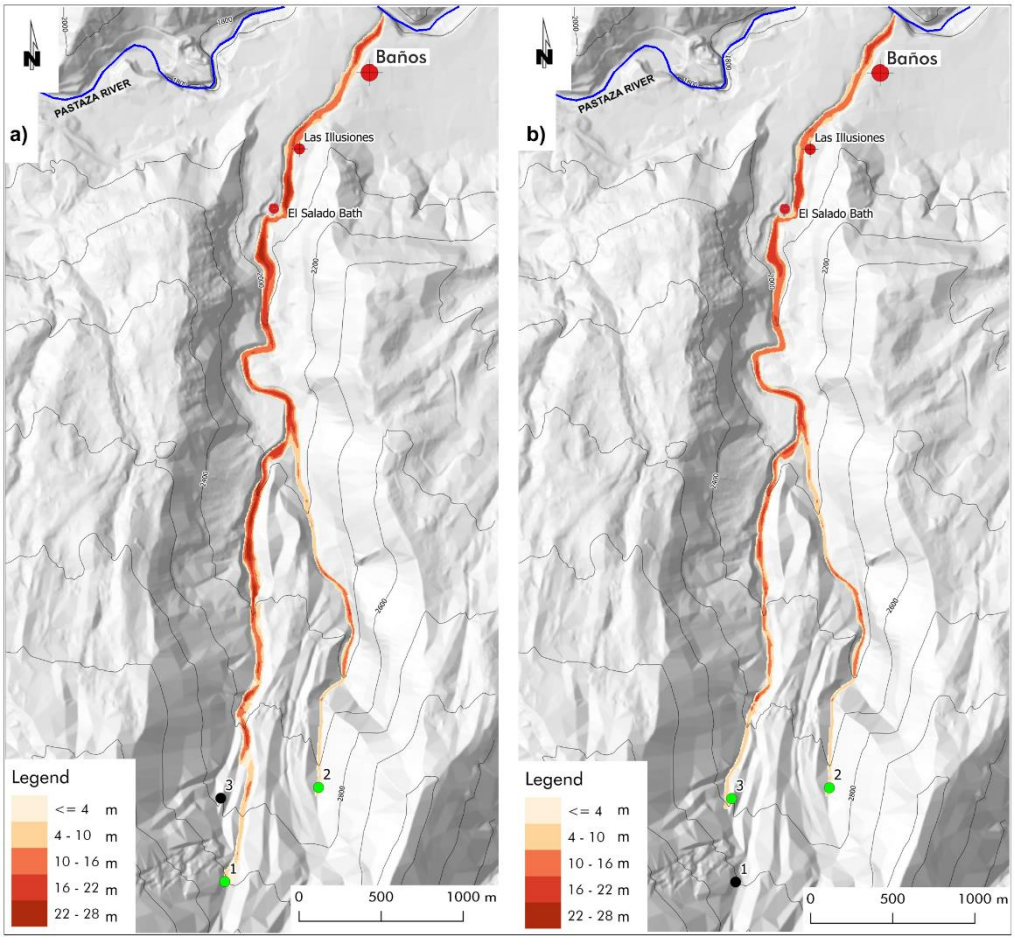

Figure 8: Simultaneous triggering of lahars from points 1 and 2 (a), from points 2 and 3 (b). The maximum thickness of the lahar during the conjectured events is reported in meters according the legend.

Initially, we considered two scenarios in order to investigate the effects of simultaneous and differed in time confluence of two lahars, the results of such simulations induced us to consider a larger set of cases. Two possible scenarios are here considered: the former one is generated by the simultaneous triggering from the points 1 with 4875 m^3 of detachment volume and 2 with 4500 m^3 of detachment volume (Fig. 8a), the second one is generated by the simultaneous triggering from the points 2 with the same previous detachment volume and 3 with 4250 m^3 of detachment volume (Fig. 8b). The confluence of

the lahars in the Rio Vascún (for the following the confluence point) is almost simultaneous in the latter scenario, because of the similar distance between the triggering points and the confluence point; the situation is diverse for the former scenario, because the distances of the triggering points from the confluence point are very different. Intuitively the former case would be less dangerous, because the flood peaks of the two lahar cannot coincide at the confluence point, but the maximum thickness of lahar in the former scenario is 27 m., while the smaller value of 21 m. is detected in the latter scenario. The analysis of the two simulations showed that a very larger mass was eroded in the first part of the path from the point 1 in the former case. This unexpected result permits to plan an opportune strategy according to the degree of control for triggering lahars 1, 2 and 3 from the three respective points. If triggering can be well controlled with moderate/heavy rainfall, then the best choice is to trigger lahar 3 (smaller erosion) before lahar 1, so that lahar 3 anticipates part of the erosion process in the common path of both the lahars (1 and 3) as far as the confluence point and reduces consequently the thickness of the lahar 1. When the peak of the lahar 3 is gone beyond the confluence point, then the lahar 2 can be triggered before the lahar 1, which has to be generated as late as possible. Anyway, the last lahar to be triggered has to be surely lahar 1 but a further investigation needs in order to understand better the priority between lahar 2 and 3; the study of single lahars generated in the points 1, 2 and 3 could solve the question, as it may be deduced with the following simulations with triggering single lahars.

Lahar 1 causes the maximum erosion, with a maximum thickness of 26 m., because it follows the path of Rio Vascún, that is the largest rio in the valley (with a larger volume of pyroclastic cover to be eroded), lahar 3 shares a relevant part of the previous path and reaches a maximum thickness of 19 m., while the lahar 2, whose path is less large before its late confluence into Rio Vascún, involves the smallest erosion (maximum thickness of 16 m). Such results solve the doubt that we put forward with the first simulations.

An operation of "cleaning" of pyroclastic cover could be projected by triggering initially lahar 2, with a first mobilization of the detrital cover as well for the area related to last part of the Rio Vascún from the confluence point of lahar 2 (maximum thickness 16 m, Fig.9b); when the lahar 2 dissolve into Pastaza river, lahar 3 could be triggered with a first erosion of the detrital cover between the confluence points of the lahars 2 and 3 into Rio Vascún, its maximum thickness does not overcome 16 m, (Fig.9c), then the most dangerous lahar 1 of Rio Vascún could start at the exhaustion of lahar 3, minimizing the hazard; the maximum thickness before the confluence of lahar 3 into Rio Vascún doesn't overcome 22 m (Fig.8a and Fig.9a).

We tested successfully the outcomes of this strategy by simulating the triggering of the three lahars in successive times, each one immediately after the exhaustion of the previous one; the first phase concerns the lahar 2 (Fig.9b), the maximum thickness doesn't overcome 14 m in the last part of the path, from north of El Salado Bath to south of Baños.

Nat. Hazards Earth Syst. Sci. Discuss., https://doi.org/10.5194/nhess-2018-406
Manuscript under review for journal Nat. Hazards Earth Syst. Sci.
Discussion started: 28 January 2019

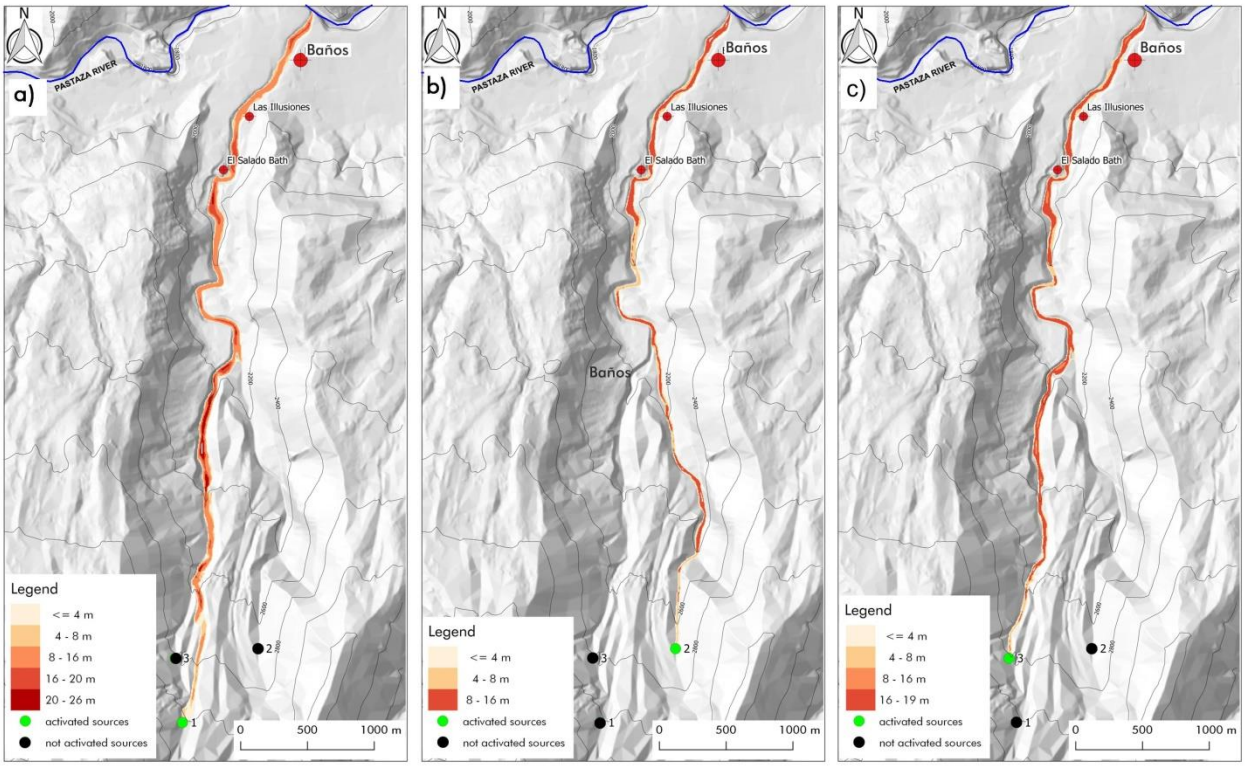

Figure 9: Single triggerings: lahar generated in point 1 (a), in point 2 (b) and in point 3 (c). The legend specifies the maximum thickness of the lahar reached during the conjectured events for each point (cell).

The erosion depth of pyroclastic cover after the lahar 2 exhaustion prevents that the maximum thickness of the successive lahar 3 overcomes 10-12 m after the confluence point with lahar 2 (Fig.10a) because of the reduced pyroclastic cover, while 19 m are reached with triggering only the lahar 3 (Fig.9c).

Finally, the most dangerous lahar 1 doesn't overcome 4-8 m in the inhabited zones (Fig.10b), while it reaches 26 m of maximum thickness in the last part of the path (Fig.9a), when the other lahars 2 and 3 are not generated.

This last result points out the importance of "cleaning" of pyroclastic cover according to an opportune strategy, that can be deduced by the outcomes of simulations, that explore all the possible significant cases.

Nat. Hazards Earth Syst. Sci. Discuss., https://doi.org/10.5194/nhess-2018-406
Manuscript under review for journal Nat. Hazards Earth Syst. Sci.
Discussion started: 28 January 2019

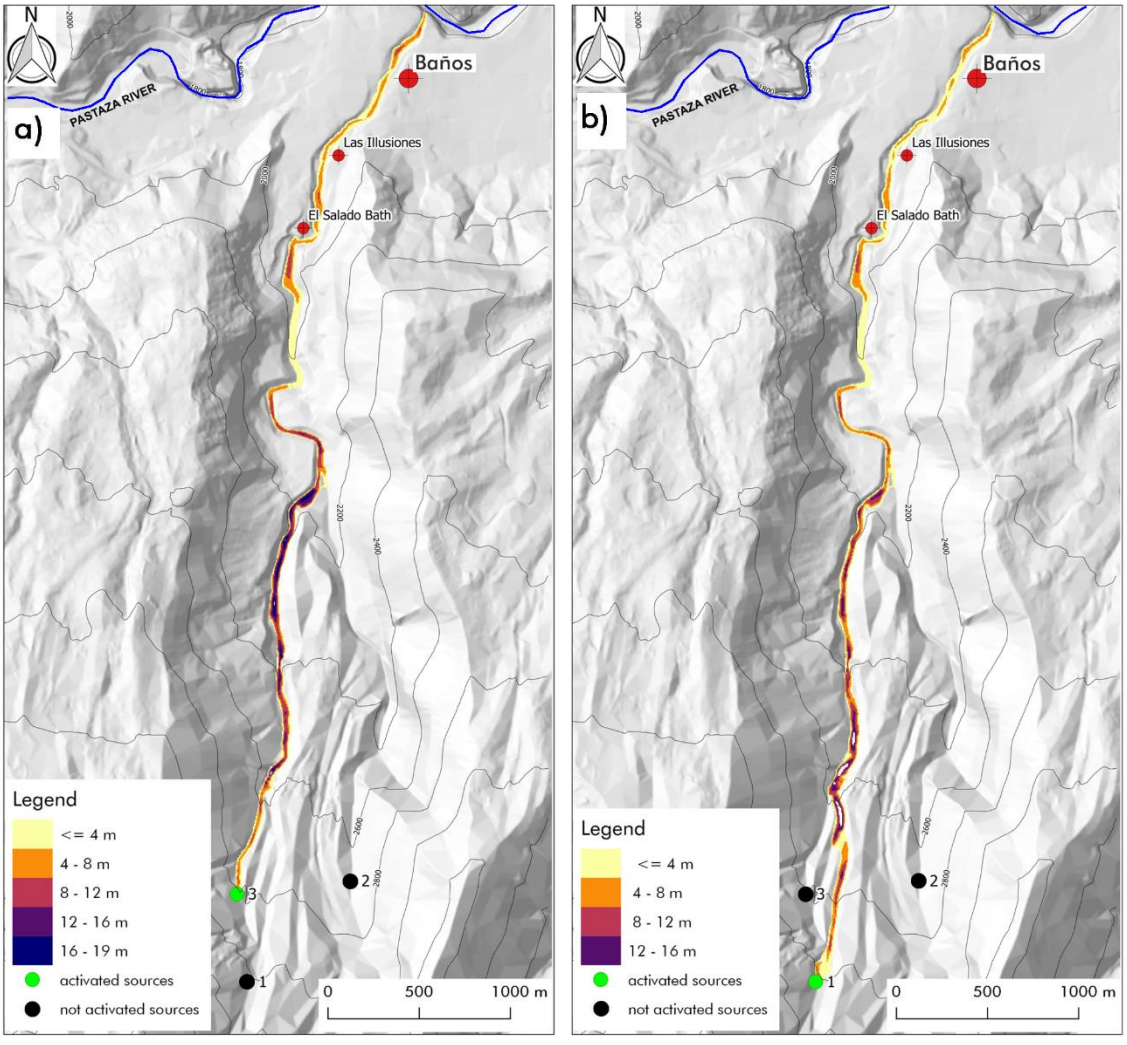

Figure 10: Simulations of deferred triggering of lahars generated in point 3 (a), and 1(b). The legend specifies the maximum thickness of the lahar reached during the conjectured events for each point (cell).

Last simulations concern two cases of simultaneous triggering of all the lahars with the same detachment volumes from points 1, 2 and 3 of the previous simulations (Fig. 11a) and the double detachment volumes from the same points (Fig. 11b) in order to understand how triggering larger volume could increase the lahar dangerousness. Results show that the maximum thickness of the lahar in the former case (Fig. 11a) is 28 m, while the maximum thickness of the lahar in the latter case (Fig. 11b) is 29 m, just a meter more. A double initial volume does not involve a much larger erosion in this context, the joint effect of a larger volume and erosion doesn't increase in dramatic way the high hazard of the situation.

The overall results confirm the goodness of the strategy of triggering lahars at different times according to an accurate analysis of simulations after a precise knowledge of the geological features of the area of application. We remember that these simulations were obtained without sufficient data about the pyroclastic cover (it is obviously overestimated) because of

Nat. Hazards Earth Syst. Sci. Discuss., https://doi.org/10.5194/nhess-2018-406
Manuscript under review for journal Nat. Hazards Earth Syst. Sci.
Discussion started: 28 January 2019

the lack of an adequate number of soil tomographies, that would have led to results with the desired precision, anyway, this problem doesn't compromise the reliability and validity of the proposed methodology.

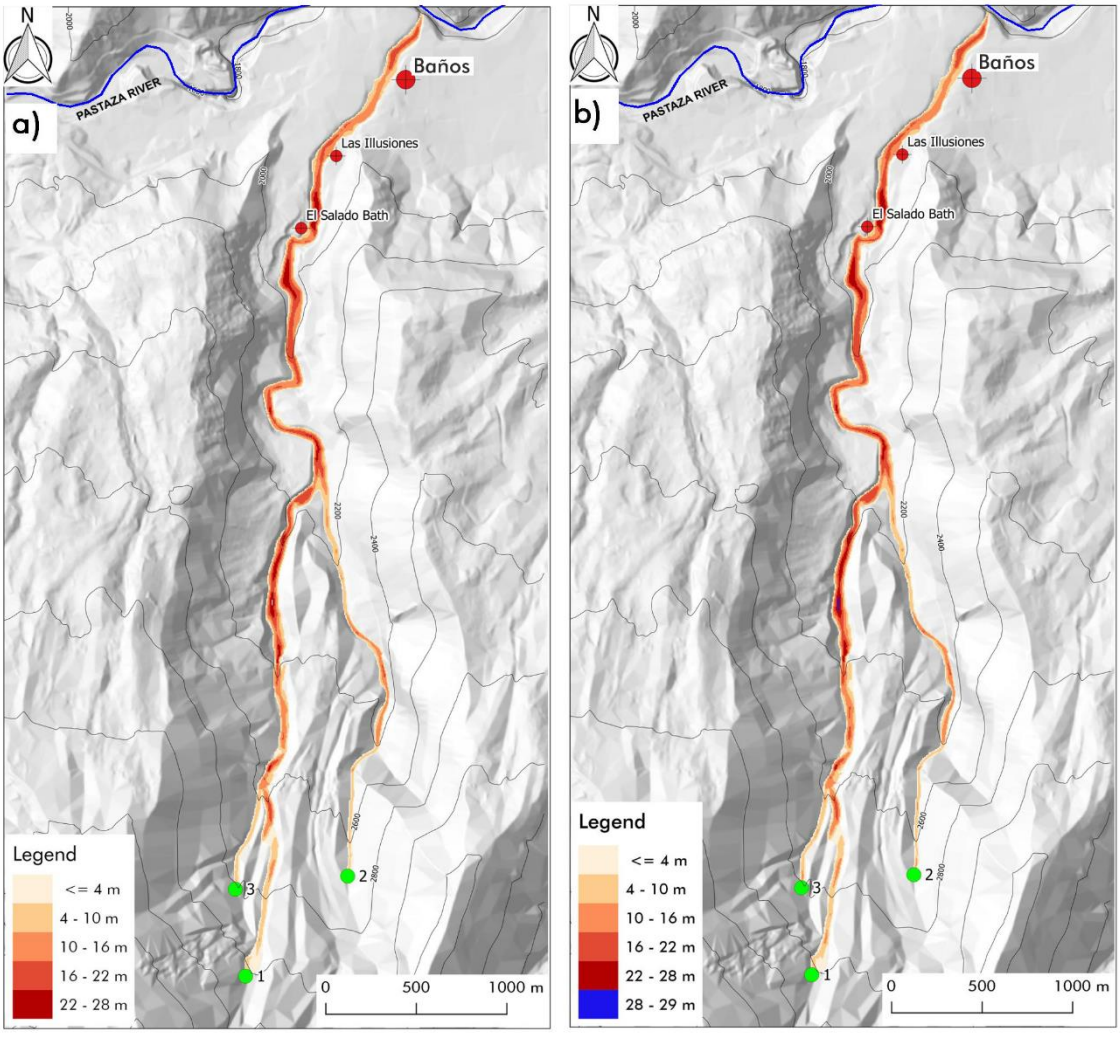

Figure 11: Simulations of simultaneous triggering of lahars generated in point 1, 2, 3. In (a) with total detachment volume of 13625 m3 and in (b) with total detachment volume of 27250 m3. The legend specifies the maximum thickness of the lahar reached during the conjectureded events for each point (cell).

5 Conclusions and comments

Our case study starts from examination of some significant natural events in the Vascún Valley, an area that is heavily exposed to lahar risk. Momentary ponds form along watercourses (rios) in the canyons of this volcanic zone, when landslides of volcanic deposits impede the normal flow. The most frequent cause of breakout of such natural ponds is the overflow of water across the newly formed dam and subsequent erosion and rapid down cutting into the loose rock debris. By eroding the

blockage and flowing out watercourse downstream, the initial surge of water will incorporate part of volcanic sediments and will generate lahars. The hazard related to these lahars depends both on the features of the temporary pond and the volcanic cover along the lahar path; a larger frequency of lahars produces smaller (shorter accumulation periods) and therefore less dangerous events.

We explored the possibility to induce artificially lahars and performed many simulations for analyzing possible different scenarios for extremely complex situations; positive results of this case study permit us to settle a methodology and encourage us to continue this investigation. We propose for risk mitigation a controlled generation of small lahars by the collapse of temporary ponds at different times in order to avoid the superposition of different lahars with the same final path. Such a proposal is out of standard and is based on observations and study of favorable situations together with the usage of a robust and well validated model of simulation in order to choose the best procedures of intervention.

The computational paradigm of Cellular Automata permitted to develop a reliable model for simulating the complex dynamics of the lahars. Reliable simulation tools permit to test various hypotheses and to create related scenarios to be analyzed.

The possibility to simulate different scenarios permits to forecast the thickness of lahars, their velocity, times of their peaks, to operate the best choice as potential hazard with more efficient and reliable alert procedures. Applications of LLUNPIY need a thorough geological study of the area of interest, especially regarding morphology (DEM and DTM), pyroclastic soil cover, the composition of the erodible layer, also specified by soil tomography at the strategic points. Furthermore, it is also important to conduct a hydrological study of watercourses, where most likely the lahar are channeled.

Feasibility studies confirmed the previous hypotheses of building weak dams with significant cost containment. Unexpected (and sometime dangerous) situations were evidenced by simulation results, which permit to evaluate the hazard of possible choices. Furthermore, more efficient and efficacious early warning protocols may be produced in such a context, social impact for partial evacuation could be mitigated. Interventions, that solve provisionally the lahar hazard, but involve future risks, can be avoided. The complexity of the objective presupposes a multidisciplinary (or perhaps transdisciplinary) approach, which implies an even greater effort to ensure those competences of different types (which are reflected by the various scientific extractions of the authors): geology, physics, mathematics, engineering, computer science can cooperate in achieving common goals. Protocols for mitigating the lahar risk can be developed in such a context, involving also social and political sciences (Leung et al., 2003).

A pilot project at least with a temporary pond needs in order to experiment in safe conditions the triggering of a small lahar. This is a preliminary step for standard applications of this new strategy for reducing the risk of lahars.

A further achievement is the extension of LLUNPIY for modelling the flows in the urbanized area as in the last versions of SCIDDICA (Lupiano et al., 2016, 2017).

Acknowledgements

This paper reports partly researches of the international project "Modelización y Simulación de Lahares con Autómatas Celulares mediante Computación Paralela" of University of Chimborazo. An indirect financial support was supplied by the University of Calabria.

References

Aguilera, E., Pareschi, M.T., Rosi, M., and Zanchetta, G.: Risk from lahars in the northern valleys of Cotopaxi Volcano (Ecuador), Nat. Hazards, 33 (2), 161–189, 2004.

Avolio, M.V., Lupiano, V., Mazzanti, P., and Di Gregorio, S.: Modelling combined subaerial-subaqueous flow-like landslides by Cellular Automata, in: ACRI 2008 (Humeo H. et al. eds.) LNCS 5191 329-336, Springer, Berlin, Heidelberg, 2008.

Avolio, M.V., Di Gregorio, S., Spataro, W., and Trunfio, G.A.: A theorem about the algorithm of minimization of differences for multicomponent cellular automata, in: ACRI 2012 (Sirakoulis G.C. and Bandini S. eds.) LNCS 7495 289-298, Springer, Berlin, Heidelberg, 2012.

Avolio, M.V., Di Gregorio, S., Lupiano, V., and Mazzanti, P.: SCIDDICA-SS3: a new version of cellular automata model for simulating fast moving landslides, J. Supercomput., 65 (2) 682–696, 2013.

Barca, D., Di Gregorio, S., Nicoletta, F.P., and Sorriso-Valvo, M.: Flow-type landslide modelling by cellular automata, in: Mesnard G., (1987, ed.) Proc. A.M.S.E. International Congress Modelling and Simulation, Cairo, Egypt, March 1987, 4A 9–15, 1986 AMSE press, Tassin-la Demi-Lune, France, 1987.

Barclay, J., Alexander, J., and Sunik, J.: Rainfall-induced lahars in the Belham Valley, Montserrat, West Indies, J. Geol. Soc. London, 164 (4) 815-827, 2007.

Biggs, J., Mothes, P., Ruiz, M., Amelung, F., Dixon, T.H., Baker, S., Hong, S.H.: Stratovolcano growth by co-eruptive intrusion: the 2008 eruption of Tungurahua Ecuador. Geophys. Res. Lett. 37, 1–5, 2010.

Bommer, J.J., Rolo, R., Mitroulia, A., Berdousis, P.: Geotechnical properties and seismic slope stability of volcanic soils, in: 12th European Conference on Earthquake Engineering, 9-13 September 2002, Barbicon Centre, London, UK, Elsevier Science, 2002.

Burgisser, A.: A semi-empirical method to calculate the permeability of homogeneously fluidized pyroclastic material, J. Volcanol. Geoth. Res., 243–244, 97–106, 2012.

Carey, M., Huggel, C., Bury, J., Portocarrero, C., and Haeberli, W.: An integrated socio-environmental framework for glacier hazard management and climate change adaptation: lessons from Lake 513, Cordillera Blanca, Peru, Climatic Change, 112(3-4), 733–767, 2012.

Chidichimo, F., De Biase, M., Rizzo, E., Masi, S., Straface, S.: Hydrodynamic parameters estimation from self-potential data in a controlled full scale site, J. Hydrol. 522, 572–581, http://dx.doi.org/10.1016/j.jhydrol.2015.01.022, 2015.

Chidichimo, F., Di Gregorio, S., Lupiano, V., Machado, G., Molina, L., and Straface, S.: Learning from nature: favoring small lahars formation for hazard mitigation, in: ENEA Proceedings of the international meeting "Relationality: between environmental awareness and societal challenges" (Fiorani L. et al., eds.) Budapest (Hungary) 87–90 ISBN: 978-88-8286-345-6, 2016.

Chidichimo, F., Mendoza, B.T., De Biase, M., Catelan, P., Straface, S., and Di Gregorio, S.: Hydrogeological modeling of the groundwater recharge feeding the Chambo aquifer, Ecuador, in: AIP Conference Proceedings 2022, 020003, doi:10.1063/1.5060683, 2018.

Chopard B. and Droz M.: Cellular automata modeling of physical systems - Cambrige University Press Collection Alea, 1998.

Córdoba, G., Villarosa, G., Sheridan, M.F., Viramonte, J.G., Beigt, D., and Salmuni, G.: Secondary lahar hazard assessment for Villa la Angostura, Argentina, using Two-Phase-Titan modelling code during 2011 Cordón Caulle eruption. Nat. Hazard. Earth Sys. Discussions, 2(10), 6373–6395, 2014.

Costa, J.E.: Hydraulic modeling for lahar hazards at Cascades volcanoes, Environ. Eng. Geosci., 3(1), 21–30, 1997.

Di Gregorio, S., and Serra, R.: An empirical method for modelling and simulating some complex macroscopic phenomena by cellular automata, Future Gener. Comp. Sy., 16 (2), 259–271, 1999.

Glickman, T.S.: Glossary of Meteorology, American Meteorological Society. MA, USA, 2000.

IGEPN: Annual Review of the Activity of Tungurahua Volcano, Technical report, Instituto Geofísico, Quito, Ecuador, www.igepn.edu.ec., 2005.

IGEPN: Informe tecnico preliminar del aluvion del 23 de agosto en el rio Vascún, http://www.igepn.edu.ec/tungurahua-informes/tung-especiales/tung-e-2008/8833-informe-especial-tungurahua-no-18/file, 2008a.

IGEPN: Weekly Report from the Tungurahua Volcano Observatory (18-24 August, 2008), Technical Report 33, Instituto Geofísico, Quito, Ecuador, www.igepn.edu.ec, 2008b.

Le Pennec, J.L., Jaya, D., Samaniego, P., Ramón, P., Moreno, S., Egred, J., van der Plicht, J.: The AD 1300–1700 eruptive periods at Tungurahua volcano, Ecuador, revealed by historical narratives, stratigraphy and radiocarbon dating, J. Volcanol. Geoth. Res., 176(1), 70–81, 2008.

Hall, M.L., Robin, C., Beate, B., Mothes, P., Monzier, M.: Tungurahua Volcano, Ecuador: structure, eruptive history, and hazards. J. Volcanol. Geoth. Res. 91, 1–21, 1999.

Iovine, G.; Di Gregorio, S.; Sheridan, M. F.; Miyamoto, H.: Modelling, computer-assisted simulations, and mapping of dangerous phenomena for hazard assessment - Environmental Modelling and Software, Volume: 22, Issue: 10, 1389-1391, 2007.

Janda, R.J., Scott, K.M., Nolan, K.M., and Martinson, H.A.: Lahar movement, effects, and deposits, US Geol. Surv. Prof. Pap., 1250, 461–478, 1981.

Janda, R.J., Daag, A.S., Delos Reyes, P.J., Newhall, C.G., Pierson, T.C., Punongbayan, R.S., Rodolfo, K.S., Solidum, R.U., and Umbal, J.V.: Assessment and response to lahar hazard around Mount Pinatubo, 1991 to 1993, in: Fire and mud: Eruptions and lahars of Mount Pinatubo, Philippines, 107–140, 1996.

Künzler, M., Huggel, C., and Ramírez, J.M.: A risk analysis for floods and lahars: case study in the Cordillera Central of Colombia, Nat. Hazards, 64(1), 767–796, 2012.

Lambe, T.W., and Whitman, R.V.: Soil mechanics, SI version, New York: Wiley, 1979.

Lane, L.R., Tobin, G.A., and Whiteford, L.M.: Volcanic hazard or economic destitution: hard choices in Baños, Ecuador, Global Environmental Change Part B: Environmental Hazards, 5(1), 23–34, 2003.

Leavesley, G.H., Lusby, G.C., and Lichty, R.W.: Infiltration and erosion characteristics of selected tephra deposits from the 1980 eruption of Mount St. Helens, Washington, USA, Hydrolog. Sci. J., 34 (3) 339–353, 1989.

Leung, M.F., Santos, J.R., Haimes, Y.Y.: Risk modeling, assessment, and management of lahar flow threat, Risk Anal., 23 (6), 1323–1335, 2003.

Lupiano, V., Avolio, M.V., Di Gregorio, S., Peres, D.J., and Stancanelli, L.M.: Simulation of 2009 debris flows in the Peloritani Mountains area by SCIDDICA-SS3, in: Proceedings of the 7th International Conference on Engineering Mechanics, Structures, Engineering Geology (EMESEG 2014), Salerno, Italy, 53–61, published by WSEAS Press, 2014.

Lupiano, V., Avolio, M.V., Anzidei, M., Crisci, G.M., and Di Gregorio, S.: Susceptibility assessment of subaerial (and/or) subaqueous debris-flows in archaeological sites, using a cellular model, in: Engineering Geology for Society and Territory, 8, 405–408, DOI: 10.1007/978-3-319-09408-3_70, Springer International Publishing Switzerland, 2015a.

Lupiano, V., Peres, D.J., Avolio, M.V., Cancelliere, A., Foti, E., Spataro, W., and Di Gregorio, S.: Use of the SCIDDICA-SS3 model for predictive mapping of debris flow hazard: an example of application in the Peloritani Mountains area, in: Proceedings of the International Conference on Parallel and Distributed Processing Techniques and Applications (PDPTA), 625–631, 2015b.

Lupiano, V., Machado, G., Crisci, G.M., and Di Gregorio, S.: A modelling approach with Macroscopic Cellular Automata for hazard zonation of debris flows and lahars by computer simulations, International Journal of Geology, 9, 35-46, ISSN: 1998–4499, 2015c.

Lupiano, V., Machado, G., Molina, L.P., Crisci, G.M., and Di Gregorio, S.: Simulations of debris/mud flows invading urban areas: a cellular automata approach with SCIDDICA, in: ACRI 2016 (El Yacoubi. et al. eds.) LNCS 9863 291–302, Springer, Berlin, Heidelberg, 2016.

Lupiano, V., Machado, G., Molina, L.P., Crisci, G.M., and Di Gregorio, S.: Simulations of flow-like landslides invading urban areas: a cellular automata approach with SCIDDICA, Nat. Comput., DOI 10.1007/s11047-017-9632-3, 2017.

Machado, G., Lupiano, V., Avolio, M.V., and Di Gregorio, S.: A preliminary cellular model for secondary lahars and simulation of 2005 case of Vascún Valley, Ecuador, in: ACRI 2014 (Wąs J. et al. eds.) LNCS 8751 208–217, Springer, Berlin, Heidelberg, 2014.

Machado, G., Lupiano, V., Crisci, G.M., and Di Gregorio, S.: LLUNPIY Preliminary Extension for Simulating Primary Lahars, in: Proceedings of the 5th International Conference on Simulation and Modeling Methodologies, Technologies and Applications, 367–376, SCITEPRESS-Science and Technology Publications, Lda, 2015a.

Machado, G., Lupiano, V., Avolio, M.V., Gullace, F., and Di Gregorio, S.: A cellular model for secondary lahars and simulation of cases in the Vascún Valley, Ecuador, J. Comput. Sci.-Neth., 11, 289–299, 2015b.

Machado, G.: Cellular Automata for Modeling and Simulating Complex Phenomena: Lahars, Case Studies of Primary and Secondary Lahars in Ecuador, PhD Thesis in Mathematics and Computer Science, Department of Mathematics and Computer Science, University of Calabria, Rende, Italy, 2015c.

Major, J., Pierson, T., Dinehart, R., and Costa, J.: Sediment yield following severe volcanic disturbance. A two-decade perspective from Mount St. Helens, Geology, 28 (9), 819–822, 2000.

Manville, V.: An overview of break-out floods from intracaldera lakes, Global Planet Change, 70,14–23, 2010.

Manville, V., Major, J.J., and Fagents, S.A.: Modeling lahar behavior and hazards, in: Modeling Volcanic Processes: The Physics and Mathematics of Volcanism, 300–330, Cambridge University Press, Cambridge, UK, 2013.

Mazzanti, P., Bozzano, F., Avolio, M.V., Lupiano, V., and Di Gregorio, S.: 3D Numerical Modelling of Submerged and Coastal Landslide Propagation, in: Submarine Mass Movements and Their Consequences, 127-139, Springer, Netherlands, 2010.

Molinari, A., Chidichimo, F., Straface, S., and Guadagnini, A.: Assessment of natural background levels in potentially contaminated coastal aquifers, Sci. Total Environ., 476–477, 38–48, 2014.

Mothes, P.A., and Vallance, J.W.: Lahars at Cotopaxi and Tungurahua Volcanoes, Ecuador: Highlights from Stratigraphy and Observational Records and Related Downstream Hazards, In: Volcanic Hazards, Risks and Disasters, edited by John F. Shroder and Paolo Papale, Elsevier, Boston, 141–168, ISBN 9780123964533, https://doi.org/10.1016/B978-0-12-396453-3.00006-X, 2015.

Muñoz-Salinas, E., Castillo-Rodríguez, M., Manea, V., Manea, M., and Palacios, D.: Lahar flow simulations using LAHARZ program: application for the Popocatépetl volcano, Mexico, J. Volcanol. Geoth. Res., 182 (1), 13–22, 2009.

O'brien, J.S., Julien, P.Y., and Fullerton, W.T.: Two-dimensional water flood and mudflow simulation, J. Hydraul. Eng., 119 (2), 244–261, 1993.

Orense, R.P., Zapanta, A.Jr., Hata, A., and Towhata, I.: Geotechnical characteristics of volcanic soils taken from recent eruptions, Geotechnical and Geological Engineering, 24, 129–161, 2006.

Pierson, T.C., Janda, R.J., Thouret, J.C., and Borrero, C.A.: Perturbation and melting of snow and ice by the 13 November 1985 eruption of Nevado del Ruiz, Colombia, and consequent mobilization, flow and deposition of lahars. J. Volcanol. Geoth. Res., 41, 17–66, 1990.

Pitman, E.B., Nichita, C.C., Patra, A., Bauer, A., Sheridan, M., and Bursik, M.: Computing granular avalanches and landslides, Phys. Fluids, 15 (12), 3638–3646, 2003.

Procter, J.N., Cronin, S.J., Fuller, I.C., Sheridan, M., Neall, V.E., and Keys, H.: Lahar hazard assessment using Titan2D for an alluvial fan with rapidly changing geomorphology: Whangaehu River, Mt. Ruapehu, Geomorphology, 116(1), 162–174, 2010.

Ramon, P., Steele, A.L., Ruiz, M.: The scientific-community interface over the fifteen-year eruptive episode of Tungurahua Volcano, Ecuador. J. Appl. Volcanol. 4 (9), 2015.

Rodolfo, K.S., Umbal, J.V., Alonso, R.A., Remotigue, C.T., Paladio-Melosantos, M.L., Salvador, J.H., Evangelista, D., and Miller, Y.: Two years of lahars on the western flank of Mount Pinatubo: Initiation, flow processes, deposits, and attendant geomorphic and hydraulic changes, in: Newhall C.G. & S. Punongbayan R.S. (1996, eds.) Fire and mud: eruptions and lahars of Mount Pinatubo, Philippines, 989–1013, University of Washington Press, Seattle and London, 1996.

Sheridan, M.F., Stinton, A.J., Patra, A., Pitman, E.B., Bauer, A., and Nichita, C.C.: Evaluating Titan2D mass-flow model using the 1963 Little Tahoma Peak avalanches, Mount Rainier, Washington, J. Volcanol. Geoth. Res., 139 (1), 89–102, 2005.

Schilling, S.P.: LAHARZ, GIS programs for automated mapping of lahar-inundation hazard zones, (No. 98-638), US Geological Survey, Information Services, 1998.

Scott, K.M.: Magnitude and frequency of lahars and lahar-runout flows in the Toutle-Cowlitz River system, US Geological Survey, Professional Paper, (USA), 1447, 1989.

Toffoli T.: Cellular Automata as an alternative to (rather than an approximation of) differential equations in modeling physics, Physica 10D, 117-127, 1984.

Vallance, J.W.: Lahars, Encyclopedia of Volcanoes, Academic Press, San Diego, CA, 2000.

Verstappen, H.T.: Volcanic hazards in Colombia and Indonesia; lahars and related phenomena, Geosciences in International Development Report, 15, 33-42, 1992.

Williams, R., Stinton, A., and Sheridan, M.: Evaluation of the Titan2D two-phase flow model using an actual event: Case study of the 2005 Vazcún Valley Lahar, J. Volcanol. Geoth. Res., 177 (4), 760-766, 2008.

Nat. Hazards Earth Syst. Sci. Discuss., https://doi.org/10.5194/nhess-2018-406
Manuscript under review for journal Nat. Hazards Earth Syst. Sci.
Discussion started: 28 January 2019

Natural Hazards and Earth System Sciences
Discussions

Table 1 - Physical and empirical parameters

Parameters	Description
p_r	cell **r**adius (half the distance between the center of the central cell and the center of one of its adjacent neighbors)
p_t	**t**ime corresponding to a MCA step
p_{cf}	**c**oefficient of **f**riction
p_{dt},	energy **d**issipation due to **t**urbulence
p_{pe} ,p_{de} , p_{tm}	**p**rogressive **e**rosion, energy **d**issipation due to **e**rosion, **t**hreshold of **m**obilization
p_{Madh}, p_{madh}	**M**ax and **m**in **adh**erence
p_{khl}	loss of kinetic head

Nat. Hazards Earth Syst. Sci. Discuss., https://doi.org/10.5194/nhess-2018-406
Manuscript under review for journal Nat. Hazards Earth Syst. Sci.
Discussion started: 28 January 2019

Natural Hazards and Earth System Sciences
Discussions

Table 2 - Substates

Substates	Description
Q_A, $Q_{D,}$	**A**ltitude, pyroclastic stratum **D**epth;
Q_{LT}, Q_{KH}	Lahar Thickness, Lahar Kinetic Head,
Q_X, Q_Y	the co-ordinates X and Y of the lahar center of mass inside the cell
Q_E, Q_{EX}, Q_{EY}, Q_{KHE} (six components)	External flow normalized to a thickness, External flow co-ordinates X and Y of mass center, Kinetic Head of External flow
Q_I, Q_{IX}. Q_{IY}, Q_{KHI} (six components)	Internal flow normalized to a thickness, Internal flow co-ordinates X and Y of mass center, Kinetic Head of Internal flow

Nat. Hazards Earth Syst. Sci. Discuss., https://doi.org/10.5194/nhess-2018-406
Manuscript under review for journal Nat. Hazards Earth Syst. Sci.
Discussion started: 28 January 2019

Natural Hazards and Earth System Sciences
Discussions

Table 3 - Comparison between field and LLUNPIY simulation data

	Field data	*LLUNPIY output*
Maximum velocity	15 m/s	20 m/s
Velocity at El Salado	4.7 m/s	6 m/s
Time between start point and El Salado bath	5’	4’ 50”
Maximum flow between start point and El Salado	640 m^3/s	633 m^3/s
Total time between start point and Rio Pastaza	-	9’
Total eroded debris	-	970000m^3